$NAE1 - 1048$

THE EFFECTS OF SMALL ICE CRYSTALS ON

THE INFRARED RADIATIVE PROPERTIES OF CIRRUS CLOUDS

Y. Takano and K. N. Liou

University of Utah, CARSS, Salt Lake City, Utah 84112

S. Asano

Meteorological Research Institute, Tsukuba, Ibaraki 305, Japan

A. Heymsfield

National Center for Atmospheric Research, Boulder, Colorado 80307

P. Minnis

Langley Research Center/NASA, Hampton, Virginia 23665

1. INTRODUCTION

To be successful in the development of satellite retrieval methodologies for the determination of cirrus cloud properties, we must have fundamental scattering and absorption data on nonspherical ice crystals that are found in cirrus clouds. Recent aircraft observations (Platt et al. 1989) reveal that there is a large amount of small ice particles, on the order of 10 μm, in cirrus clouds. Thus it is important to explore the potential differences in the scattering and absorption properties of ice crystals with respect to their sizes and shapes. In this study the effects of nonspherical small ice crystals on the infrared radiative properties of cirrus clouds are investigated using light scattering properties of spheroidal particles.

In Section 2, using the anomalous diffraction theory for spheres and results from the exact spheroid scattering program, efficient parameterizatation equations are developed for calculations of the scattering and absorption properties for small ice crystals. Parameterization formulas are also developed for large ice crystals using results computed from the geometric ray-tracing technique and the Fraunhofer diffraction theory for spheroids and hexagonal crystals. This is presented in Section 3. Finally, applications to the satellite remote sensing are described in Section 4.

2. PARAMETERIZATION FOR SMALL ICE CRYSTALS

Because the effects of nonsphericity would be small in the infrared region, small ice crystals may be approximated as spheroidal particles. For small size parameters of spheroidal particles,

scattering parameters computed from the Mie theory are adjusted to match with those computed exactly by the method of Asano and Sato (1980) based on the anomalous diffraction theory (Latimer 1980).

For a spheroid of semi-axes a_e and va_e, the equivalent spherical radius is given by

$$a_s = a_e \left[v/(\cos^2\zeta + v^2 \sin^2 \zeta)^{1/2}\right]^{k_1} , \qquad (1)$$

where ζ is the angle between the incident direction and the rotation axis of the spheroid, a_e the radius of the revolved circle, and v the axial ratio. The extinction or scattering cross section of the spheroid is given by

$$C(\zeta) = Q_{sph} \, \pi a_e^2[(\cos^2\zeta + v^2 \sin^2\zeta)^{1/2}]^{k_2} , \qquad (2)$$

where Q_{sph} is the optical efficiency factor from the Mie theory for a sphere of radius, a_s, and refractive index, $m (= m_r - i\, m_i)$. If k_2 is 1 in Eq. (2), the right-hand side becomes Q_{sph} times the geometric shadow area of the spheroid. The cross section for randomly oriented spheroids is expressed by

$$\bar{C}_{e,s} = \int_0^{\pi/2} C_{e,s} \, (\zeta)\sin \zeta \, d\zeta . \qquad (3)$$

The unknown constants, k_1 and k_2, in Eqs. (1) and (2) are determined by matching $\bar{C}_e/\bar{A}$, where $\bar{A}$ is the average geometric cross section of the spheroid, with that computed exactly by Asano and Sato (1980) as follows:

$$\left.\begin{aligned} k_1 &= 1.0, & k_2 &= 0.98, & for\ v{\geq}1 , \\ k_1 &= 0.96, & k_2 &= 1.08, & for\ v{<}1 . \end{aligned}\right\} \qquad (4)$$

Further, by comparing with values computed from the method of Asano and Sato, the extinction cross section for randomly oriented spheroids may be expressed by

$$
C_e = \begin{cases} \bar{C}_s + C_{a,ves}, & \text{for } m_i < 0.07 , \\ \bar{C}_e, & \text{for } m_i \geq 0.07 . \end{cases} \tag{5}
$$

where $C_{a,ves}$ is the absorption cross section for the volume equivalent sphere. The single scattering albedo is given by

$$
\bar{\omega} = \frac{\bar{C}_s}{\bar{C}_s + C_{a,ves}} . \tag{6}
$$

When the spheroid shape becomes flat or elongated, scattered light rays are inclined toward forward directions. This effect on the asymmetry factor is mimicked by adjusting the refractive index and size.

With this procedure, the single scattering properties of randomly oriented spheroids can be efficiently calculated. Figures 1 (a) and 1 (b) show the single scattering properties of randomly oriented oblate and prolate spheroids with the axial ratio of 2 as a function of $x_G = 2\pi r_G/\lambda$ for 11 and 12 μm wavelengths, where r_G is the radius of area-equivalent spheres. The solid and dash-dotted lines are calculated by means of the preceding parameterization. Circles and crosses are values computed exactly from the method of Asano and Sato. The accuracy of the present parameterization is within about 3%.

3. PARAMETERIZATION FOR LARGE ICE CRYSTALS

For large size parameters we use the geometric optics approximation to develop parameterization equations. The single scattering properties of spheroids are computed from the ray-tracing method and Fraunhofer diffraction theory. Using these computed values, parameterized formulas for the single scattering properties of large ice crystals are derived.

Figure 2 shows the scattering phase functions for randomly oriented oblate spheroids with the axial ratio, $1/v = 2$, and $m = (1.33, 0)$ computed from the ray-optics approximation and the exact method. The size parameter used is 30, which is twice the value used in Fig. 9 of Asano and Sato (1980). The peaks at the 0° scattering angle that are produced by the Fraunhofer diffracted light have about the same values for the two methods. The peak appeared at $\theta = 76°$, computed from the ray-optics approximation, corresponds to the maximum created by one internal reflection (primary rainbow feature). Since the rainbow angle is dependent on the incident direction on the spheroid, the rainbow peak is smaller than that of spheres. Based on the exact method the rainbow angle is located at about $\theta = 94°$. The peak is smaller and broader and shifts toward backward direction. This behavior is the same as that in the case of spheres (Liou and Hansen 1971) and circular cylinders (Takano and Tanaka 1980). Glory-like peaks appear at the backward direction ($\theta = 180°$) on both methods. If the size parameter is larger, these two methods give closer values. This comparison verifies the ray-tracing program developed in the present research and the Fraunhofer diffraction approach developed by Takano and Asano (1983). Hence, it is possible to para-
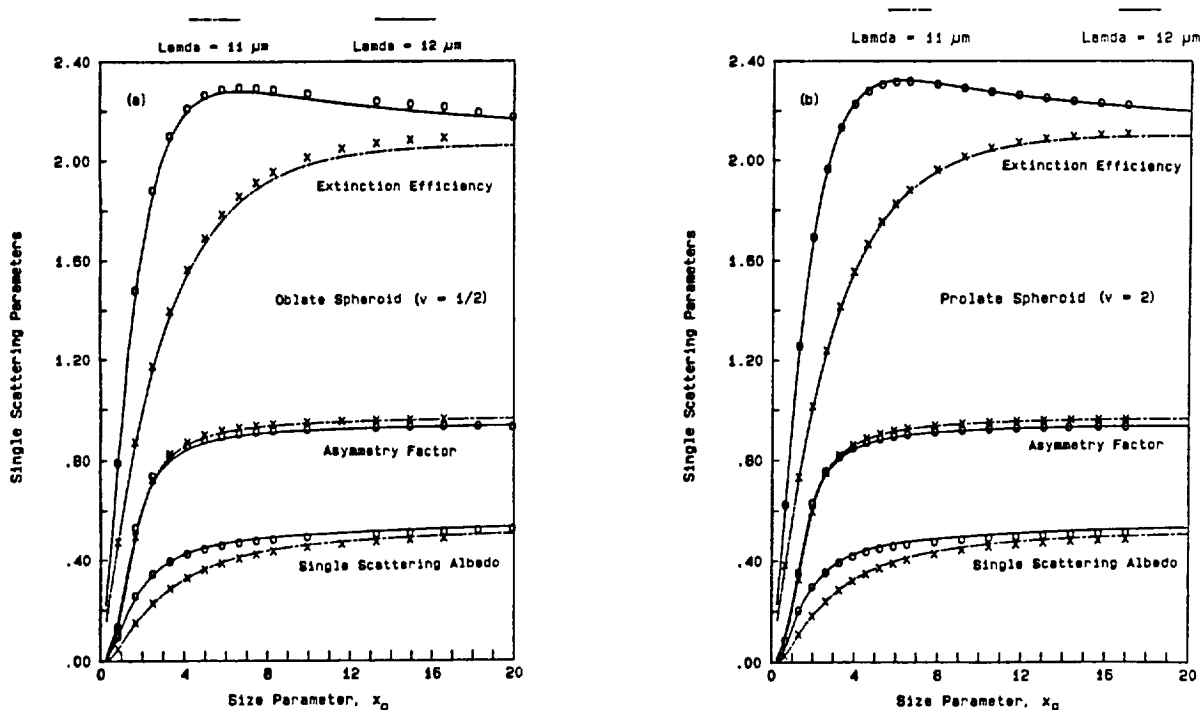

Fig. 1: Comparison of single scattering properties for randomly oriented (a) oblate and (b) prolate spheroids between the parameterization (solid and dash-dotted lines) and the exact computation (circles and crosses). The complex refractive indexes of ice used are $m = 1.0925-i0.2480$ at $\lambda = 11$ μm and $m = 1.280-i0.4133$ at $\lambda = 12$ μm.
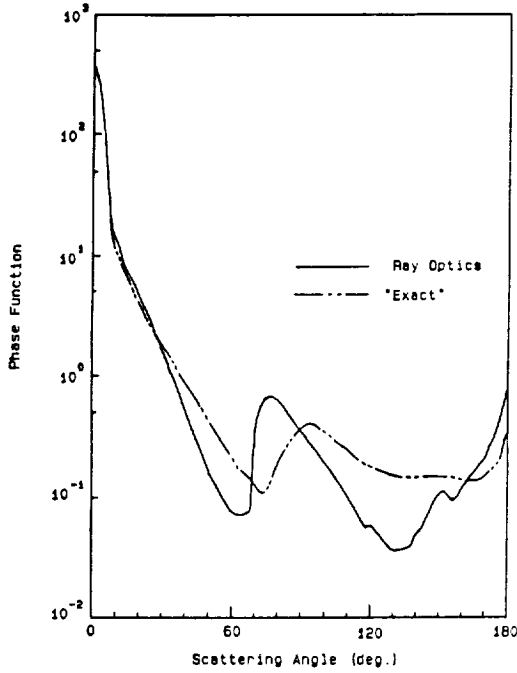
Fig. 2: Comparison of the phase function for randomly oriented oblate spheroids using the ray-optics approximation (solid line) and the exact theory (dash-dotted line). The axial ratio, the complex refractive index, and the size parameter used are 2, (1.33, 0) and 30, respectively.

meterize the single scattering albedo and asymmetry factor of large spheroids using these programs.

When absorption in a spheroidal particle is weak, the absorption cross section can be expressed by

$$C_a \propto \frac{4\pi m_i}{\lambda} \, r_v^3 \, , \tag{7}$$

where m_i is the imaginary index of refraction and r_v the radius of the volume equivalent sphere. Thus, the absorption efficiency is given by

$$Q_a = \frac{C_a}{\pi r_G^2} \propto \frac{4\pi m_i}{\lambda} \frac{r_v^3}{r_G^2} = z \, . \tag{8}$$

The single scattering co-albedo may then be expressed by

$$1 - \bar{\omega} = \frac{Q_a}{2} = \sum_{n=1}^{N} a_n z^n \, . \tag{9}$$

Using values of $\bar{\omega}$ computed by the ray optics approximation for a number of z, the coefficients, a_n, are determined. Figure 3 (a) shows the single scattering co-albedo for randomly oriented oblate spheroids as a function of z. The solid line is calculated from Eq. (9), whereas symbols (o, +, and x) are computed from the ray-optics approximation. The fitting is sufficiently accurate in the range of $z \leq 0.4$. On the other hand, when absorption dominates, the single scattering co-albedo should approach to a constant value, which cannot be expressed by Eq. (9). Using the anomalous

diffraction formula for spheres, the single scattering albedo for intensively absorbing spheroids may be written in the form

$$\bar{\omega} = 1 - (1 - \bar{\omega}_\infty) \, 2 \, K(cz) \, , \tag{10}$$

where

$$K(w) = \frac{1}{2} + \frac{e^{-w}}{w} + \frac{e^{-w}-1}{w^2} \, . \tag{11}$$

As a result, $\bar{\omega} = 1$ when $z = 0$, and $\bar{\omega} = \bar{\omega}_\infty$ when $z \longrightarrow \infty$. To be consistent with Eq. (9), z is chosen as the independent variable. The constant, c, in Eq. (10) should be determined by fitting this formula with ray-optics computations. $\bar{\omega}_\infty$ in Eq. (10) is given by $Q_{sca,\infty}/2$. $Q_{sca,\infty}$ is 1 plus the external reflected energy. Figure 3 (b) shows the single scattering co-albedo as a function of z (> 0.4). The constant in Eq. (10) depends on the axial ratio of spheroid.

The extinction efficiency is given by

$$Q_e(x) = 2 + \frac{x_c}{x} \, [Q_e(x_c) - 2] \, . \tag{12}$$

With this functional form, $Q_e = 2$ when $x \longrightarrow \infty$ and $Q_e = Q_e(x_c)$ at the crossover point, x_c. The crossover point is the size parameter which separates small and large particle regions. The crossover point is determined in the following manner.
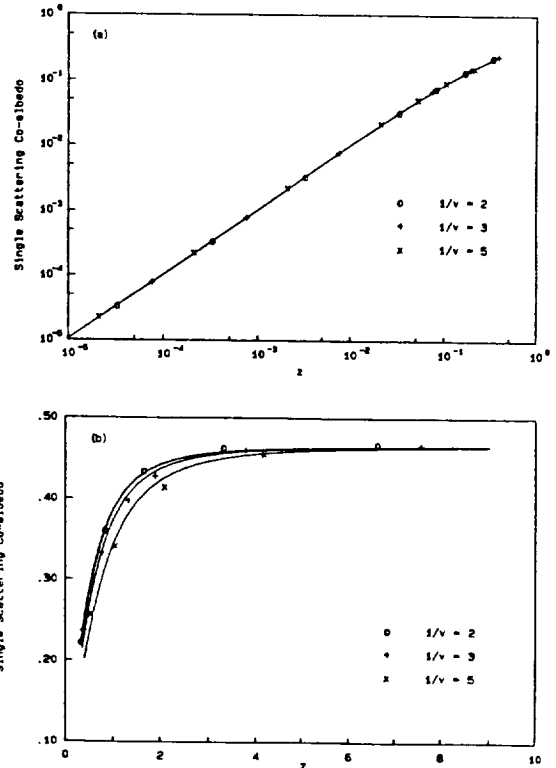

Fig. 3: Single scattering co-albedo for randomly oriented oblate spheroids as a function of z for (a) weak and (b) strong absorption. The assumed axial ratios are 2, 3, and 5, which are represented by o, +, and x, respectively.

Figures 4 (a) and 4 (b) show the composite single scattering albedo for randomly oriented oblate and prolate spheroids with the axial ratio of 2 as a function of the size parameter, x_a, at a wavelength of 11 µm. The solid lines are the large particle parameterization using Eqs. (9) and (10), whereas the dot-dashed lines are the small particle parameterization using Eq. (6). For comparison purposes, the values computed by the exact method are represented by circles. From these figures the crossover point, x_c, is about 22 in units of the area equivalent size parameter. A similar procedure can be applied to the asymmetry factor.

For size parameters larger than about 30, parameterization equations have been derived using the results computed from the geometric ray-tracing technique for hexagonal crystals (Takano and Liou 1989; Liou et al. 1990). The extinction cross section for randomly oriented hexagonal crystals of the same size can be expressed by

$$C_e = \frac{3}{2}(\frac{w}{2})^2 (\sqrt{3} + \frac{4D}{w}) , \qquad (13)$$

where w is the width of the basal plane of a hexagonal crystal and D the crystal maximum length. Based on numerical calculations involving a number of wavelengths, particle sizes, D, and aspect ratio, D/W, we find that the single scattering albedo can be parameterized in the form:
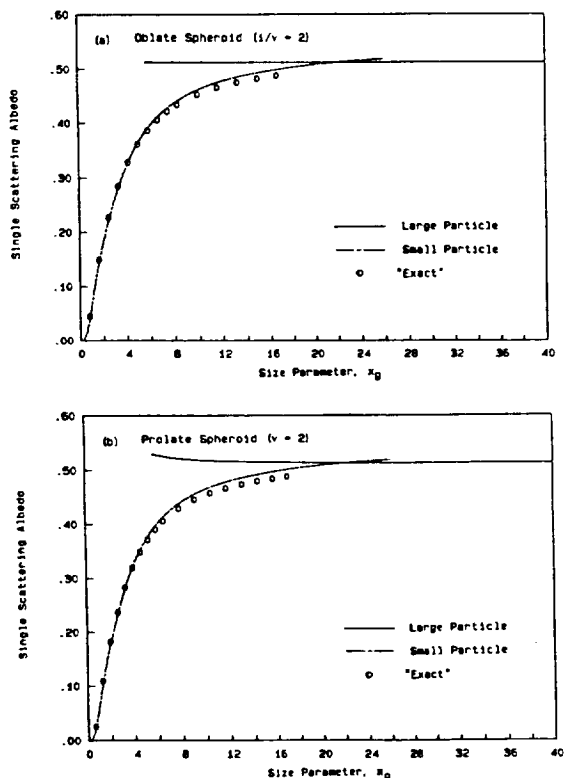

$$\tilde{\omega} = \begin{cases} 1 - \sum_{n=1}^{4} f_n z^n , & for\ z < 0.4 , \\ & \qquad\qquad (14) \\ 1 - 0.47 [1 - \exp(-1.5051 z^{0.6789})] , & for\ z \geq 0.4 , \end{cases}$$

where z is a physical parameter defined by

$$z = \frac{4\pi m_i}{\lambda} \frac{r_v^3}{r_G^2} = \frac{4\pi m_i}{\lambda} \frac{w}{2} \frac{3\sqrt{3}}{\sqrt{3} + 4(D/w)} \frac{(D/w)}{} . \qquad (15)$$

The coefficients in Eq. (14) are: $f_1 = 1.1128$, $f_2 = -2.5576$, $f_3 = 5.6257$, and $f_4 = -5.9498$.

4. APPLICATION TO SATELLITE REMOTE SENSING

Using these parameterizations, the scattering and absorption properties for ice crystal size distributions obtained during the FIRE Intensive Field Observation and the effects of small ice crystals on the infrared radiative properties are examined. As shown in Fig. 1, the absorption efficiencies of ice crystals for the wavelengths of 11 and 12 µm can differ by as much as a factor of two. This could provide a means for the detection of small ice crystals using the radiances measured from AVHRR channels 4 and 5.

5. ACKNOWLEDGEMENTS

6. REFERENCES

Asano, S. and M. Sato, 1980: Light scattering by randomly oriented spheroidal particles. Appl. Opt., 19, 962-974.

Latimer, P., 1980: Predicted scattering by spheroids: Comparison of approximate and exact methods. Appl. Opt., 19, 3039-3041.

Liou, K.N. and J.E. Hansen, 1971: Intensity and polarization for single scattering by polydisperse spheres: A comparison of ray-optics and Mie theory. J. Atmos. Sci., 28, 995-1004.

Liou, K.N., Y. Takano, S.C. Ou, A. Heymsfield, and W. Kreiss, 1990: Infrared transmission through cirrus clouds: A radiative model for target detection. Appl. Opt. (in press).

Platt, C.M.R., J.D. Spinhirne, and W.D, Hart, 1989: Optical and microphysical properties of a cold cirrus cloud: Evidence for regions of small ice particles. J. Geophy. Res., 94, 11151-11164.

Takano, Y. and S. Asano, 1983: Fraunhofer diffraction by ice crystals suspended in the atmosphere. J. Meteor. Soc. Japan, 61, 289-300.

Takano, Y. and K.N. Liou, 1989: Solar radiative transfer in cirrus clouds. Part I: Single-scattering and optical properties of hexagonal ice crystals. J. Atmos. Sci., 46, 3-19.

Takano, Y. and M. Tanaka, 1980: Phase matrix and cross sections for single scattering by circular cylinders: A comparison of ray optics and wave theory. Appl. Opt., 19, 2781-2793.

Fig. 4: *Single scattering albedo for randomly oriented (a) oblate and (b) prolate spheroids with the axial ratio of 2 at a wavelength of 11 µm computed from the large particle parameterization (solid line), the small particle parameterization (dash-dotted line), and the exact method (circles).*